Biomedical Microdevices (2021) 23: 13
https://doi.org/10.1007/s10544-021-00554-3

Development of a sandwich-type rat small intestine tissue sensor for detecting resveratrol and its receptors

Ruijuan Ren[1] · Dingqiang Lu[1,2] · Tingting Liu[1]

Accepted: 22 February 2021 / Published online: 5 March 2021

Abstract
Resveratrol has a variety of biological functions, however, a limited number of studies have assessed its interaction with cell surface receptors. In this study, a sandwich-type rat small intestine tissue sensor (RSIT-sensor) was fabricated to detect the response current from receptor stimulation by different resveratrol concentrations via electrochemical workstation. The results showed that with detection limit of 1×10^{-13} mol/L, the maximum rate of change of the response current was found at the concentration of 8.5×10^{-12} mol/L, indicating that the resveratrol-related receptor was saturated. With comparing the response values of prepared biosensor and bare electrode with resveratrol, it can be concluded that the response value of small intestinal cells to resveratrol has obviously been amplified by the intracellular signal transmission system, and its magnification was about 100 times. In the current research, for the first time, kinetics of the interaction between resveratrol and its receptors and the transmission of signals to the body could be quantitatively measured by a biosensor. Our findings may provide new ideas for resveratrol-related receptor analysis, separation and purification, signal transmission, and evaluation of biological function.

Keywords Electrochemical biosensor · Resveratrol · Rat small intestine · Sandwich-type membrane · Receptor-ligand interaction

1 Introduction

Resveratrol (3,5,4′-trihydroxy-trans-stilbene) is a polyphenol phytoalexin present in a variety of plant species and has been implicated to explain the health benefits of red wine. A wide range of health beneficial effects have been reported for resveratrol in animal studies (Jang et al. 1997; Tsai et al. 2017; Ahmad and Hoda 2020; Diaz-Gerevini et al. 2016). Previous studies demonstrated that resveratrol has biological pharmacological activities that are beneficial to human health in various aspects, such as anti-cancer (Kim et al. 2016), anti-cardiovascular disease (Elshaer et al. 2018), treatment of diabetes (Öztürk et al. 2017), anti-mutation (Bhullar and Udenigwe 2016), antibacterial (Bostanghadiri et al. 2017), anti-inflammation (Poulsen et al. 2015), antioxidant properties (Ndiaye et al. 2011), inducing apoptosis (Oliveira et al. 2016), relieving metabolic disorders (Ligt et al. 2015), etc. Although resveratrol has been widely used as a health care product, a limited number of studies quantitatively described the degree of intracellular signal amplification caused by the interaction between resveratrol receptor and ligand (Kulkarni and Cantó 2015). A number of direct and indirect target molecules mediating the aforementioned cardiovascular effects of resveratrol have been identified. These include nuclear factor-κB (NF-κB), AP1, the estrogen receptor-α (ER-α), the adenosine receptors, the cyclooxygenase 1, the AMP-activated protein kinase (AMPK), and the histone/protein deacetylase sirtuin 1 (Li et al. 2012; Athar et al. 2009). Studying the dynamics of the action of resveratrol and its receptors can be helpful for exploration of the effects of resveratrol on the body, and it can better highlight the therapeutic effects of resveratrol on human health.

Studies have shown that resveratrol can reduce intestinal damage and improve the intestinal barrier integrit (Sandoval-Ramírez et al. 2020). The small intestine epithelium, as

Ruijuan Ren and Tingting Liu are equally contributed to this work

✉ Dingqiang Lu
dqlu@tjcu.edu.cn; m18222368363@163.com

[1] College of Biotechnology & Food Science, Tianjin University of Commerce, Tianjin 300314, China

[2] Tianjin Key Laboratory of Food Biotechnology, Tianjin 300314, China

a medium for the internal and external environment of the intestine and an important part of the body's immune barrier, has a variety of biological functions, such as digestion, absorption, and secretion (Allaire et al. 2018; Vojdani et al. 2020). Resveratrol is not easily absorbed from the gut it is likely that it may act on endocannabinoid and light, odor, and taste receptors located in the gut, which, in turn, convey their messages to the various organs via vagus nerve (Repossi et al. 2020). Therefore, resveratrol could activate several extracellular targets on the small intestinal epithelium to transmit regulatory signals to the body to play a healthy function. The present study, for the first time, developed an electrochemical biosensor using rat small intestine tissue as a sensitive element to detect resveratrol. In the present study, a small intestine tissue was fixed between two nuclear microporous membranes, and then, connected with the glassy carbon electrode (GCE) to fabricate an electrochemical biosensor. When the small intestine tissue sensor contacts with the resveratrol solution, it may cause electrochemical changes. After that, the electrical signal can be measured by an electrochemical workstation. The change of electrical signal can be used to quantitatively detect the resveratrol and the interaction between resveratrol and its receptor (Wei et al. 2017; Xu et al. 2019).

The traditional method for studying the action of ligand receptors is to purify the receptors separately, while the process of purifying the receptors is relatively difficult. Moreover, when the receptor leaves the cell membrane, it often loses the anchoring effect of the membrane and the role of some intracellular cofactors, while it does not truly reflect the actual conformation of the receptor on the cell membrane and its role with the ligand (Venkatakrishnan et al. 2013; Ushiama et al. 2016). Using small intestine tissue cells as sensitive elements and effectors, they can well maintain the biological structure of the resveratrol receptor protein and the cellular microenvironment. Small intestinal tissue cells interact with resveratrol to activate the intracellular signal transduction system and transmit physiological and electrochemical signals (Ye et al. 2019; Martins et al. 2012; Méjard et al. 2014; Qiao et al. 2015; Xiao et al. 2019). In addition, the resveratrol concentration and receptor interaction curve can be obtained through the current change rate, and the ligand-receptor binding constant and dissociation constant can be indirectly achieved, and then, the kinetics can be studied. Our results may provide a new idea and evaluation method for the study of ligand-receptor interaction.

2 Materials and methods

Nucleopore membrane was obtained from GE Whatman (Buckinghamshire, UK). Soluble starch was purchased from Tianjin Yingdaxi Co., Ltd. (Tianjin, China). Sodium alginate was provided by Tianjin Guangfu Fine Chemical Research Institute (Tianjin, China). Glutaraldehyde was purchased from Tianjin Bodi Chemical Engineering Co., Ltd. (Tianjin, China). Bovine serum albumin (BSA) was provided by Ye Xiang Bio. Co., Ltd. (Hangzhou, China). Phosphate-buffered saline (PBS; pH 7.0) was purchased from Thermo Fisher Scientific (Waltham, MA, USA). $CaCl_2$ and resveratrol were obtained from Sigma-Aldrich (St. Louis, MO, USA). All reagents were of analytical grade, and ultrapure water was applied.

The electrochemical experiments were performed using the CHI660E electrochemical workstation provided by Chenhua Co., Ltd. (Shanghai, China), equipped with a three-electrode system consisting of GCE as the working electrode, Ag/AgCl as the reference electrode, and platinum-wire electrode as the counter electrode. The ultrapure water was prepared by Millipore Milli-Q water purifier (Shanghai Yarong Biochemical Equipment and Apparatus Co., Ltd., Shanghai, China). KQ 3200B ultrasonic cleaner was purchased from Kun Shan Ultrasonic Instruments Co., Ltd. (Hangzhou, China) was used for electrode pretreatment. DHG-907385-III CIMO electric constant temperature drying oven was supplied by Shanghai Xinmiao Medical Device Manufacturing Co., Ltd. (Shanghai, China), and was used for the drying of electrode modification process.

Besides, Sprague–Dawley (SD) rats (age, 8 ~ 10 weeks; body weight, 240 ~ 270 g) were provided by Tianjin Xiangtian Technology Co., Ltd. (Tianjin, China).

2.1 Preparation of rat small intestine tissue sensor (RSIT-sensor)

Take the ileal segment (1 cm) in the middle of the rat small intestine, wash the contents, cut the small intestine segment into a plane with a razor blade, take 0.25 cm^2 of the small intestine plane, and put it in saline for use. Before the assembly of the RSIT-sensor, the GCE was pre-treated by conventional methods. As described previously (Wei et al. 2017; Xu et al. 2019), using sodium alginate-starch gel as a fixing agent, small intestine tissues of SD rats were fixed between two nuclear micro porous membranes, forming a sandwich-type membrane, and then fixed to a glassy carbon electrode to make a biosensor electrode. The sandwich-type RSIT-sensor was fabricated to detect the response current from receptor stimulation by different resveratrol concentrations. Figure 1 shows the assembly and working principle of the proposed biosensor. The detection principle is that the binding of resveratrol to the receptors causes the small intestine cells to Ca^{2+}-mediated apoptosis. The detection principle is that the binding of resveratrol to the receptor may lead to Ca^{2+}-mediated apoptosis of small intestinal cells (Subramanian et al. 2010). Apoptosis causes a large

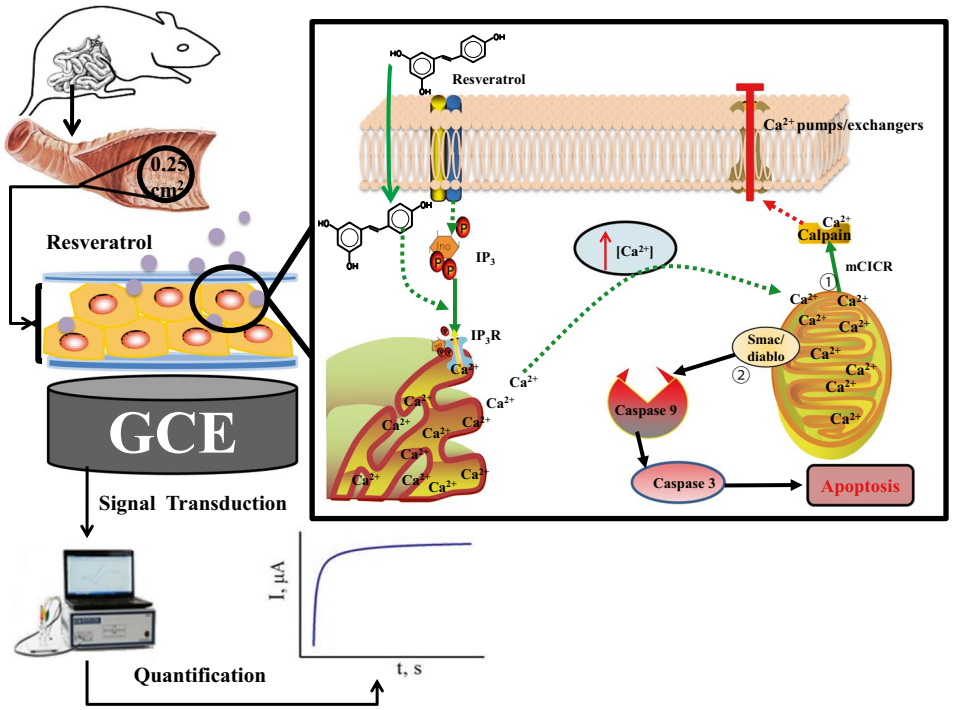

Fig.1 Assembly and working principle of the sensor

amount of intracellular contents to be released into the test solution, which causes changes in electrical signals. The RSIT-sensor simulates organisms by transferring the electrical signal to the computer to display the interaction between receptor and ligand.

When the small intestine tissue sensor contacts with the resveratrol solution, resveratrol activates the inositol triphosphate receptor (IP3R) either through an extracellular receptor or through an intracellular target resulting in release of extracellular receptor calcium, reflected in a rapid increase in intracellular calcium. The subsequent calcium uptake by the mitochondria causes mitochondrial membrane depolarization, release of smac/diablo, activating the intrinsic apoptotic pathway via caspases-9 and -3. Mitochondrial calcium-induced-calcium-release (mCICR) results in the activation of calpain, which then cleaves various substrates including calcium exchangers and pumps, leading to additional elevation of intracellular calcium, further stimulating cell death (Subramanian et al. 2010).

2.2 Detection of resveratrol by the RSIT-sensor

Amperometry was used to detect the response currents of different concentrations of resveratrol diluted with 0.9% NaCl under the optimized voltage by the RSIT-sensor. Using 0.9% NaCl as a blank control and the change rate of response current as the detection index, the response curve of current change rate to resveratrol was formulated. The equation for calculation of ΔI is as follows:

$$\Delta I/\% = \frac{I_1 - I_2}{I_1} \times 100 \quad (1)$$

where, I_1 and I_2 refer to the steady-state current value at the same time point when resveratrol concentration was estimated before and after measurement, respectively. When the difference between the response current value of the test bottom solution (Control) and the test solution was close to zero, the concentration of the test substance at this time was measured three times in parallel at each concentration.

3 Results and discussion

3.1 Fabrication and characterization of the RSIT-sensor

As reported previously (Ren et al. 2020), cyclic voltammetry (1 mM $K_3Fe(CN)_6$ containing 0.20 mol/L KNO_3, scan range: 0.6 ~ -0.1 V, scan rate: 50 mV/s) was used to characterize the performance of GCE. As illustrated in Fig. 2a, the peak potential difference is below 80 mV, and the redox peak current ratio is close to 1. In addition, as shown in Fig. 2b, the redox peak current has a proper linear correlation with the square root of the scan rate (25 ~ 200 mV/s). The above-mentioned results indicated that the surface of the GCE could be only controlled by diffusion after pretreatment. The pretreatment effect of the GCE met the requirements of subsequent experiments.

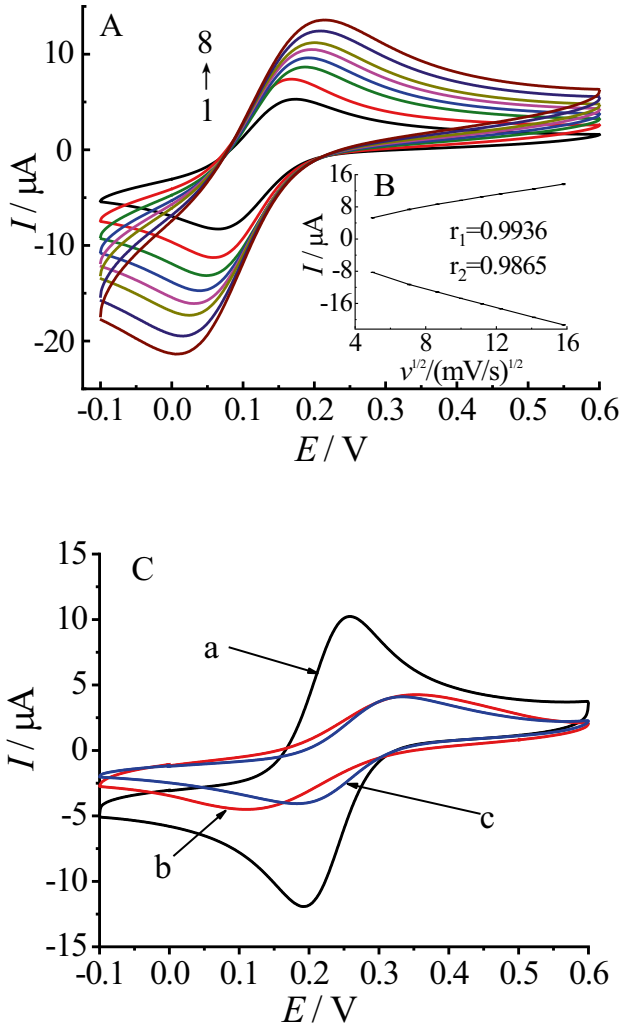

Fig. 2 (**a**) Cyclic voltammograms of bare GCE after pretreatment at the scan rate: 25 ~ 200 mV/s (1 → 8); the inset (**b**) shows the dependence of the redox peak currents on the square root of scan rates; (**c**) Characterized electrode at different modification stages by cyclic voltammetry. **a**, **b**, and c represent bare GCE, nucleopore membrane-GCE, and rat small intestine tissue-nucleopore membrane-GCE, respectively. (**a**), (**b**) and (**c**) were performed in1 mM $K_3Fe(CN)_6$ containing 0.20 mol/L KNO_3

Figure 2c displays the characterizations of different stages of fabrication of RSIT-sensor in 1 mM $K_3Fe(CN)_6$ solution (containing 0.20 mol/l KNO_3) by cyclic voltammetry. The curves a, b, and c in Fig. 2c respectively represent three different modification phases for GCE, nucleopore membrane-GCE, and rat small intestine tissue-nucleopore membrane-GCE. After assembling the nucleopore membrane and rat small intestine tissue on the electrode surface, the peak current continuously decreased due to the obstruction of electron transmission. It was unveiled that the sensor could be stably combined with the sandwich tissue membrane. However, the performance of the RSIT-sensor needs to be further tested.

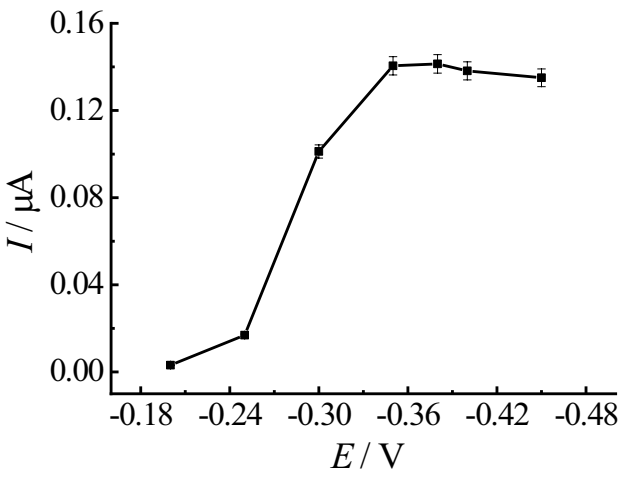

Fig. 3 The rate of change of the response current of the RSIT-sensor under different voltage values

3.2 Optimization of amperometry

The prepared sensor was tested by Amperometry under different potential conditions (saline was used as the blank control). There were differences in steady-state current values before and after addition of 10^{-5} mol/L resveratrol. The results demonstrated that the maximum variation of current values was observed at -0.38 V (Fig. 3). Therefore, -0.38 V was taken as the constant potential into account for probing the response characteristic of the biosensor to resveratrol.

3.3 Regularity of resveratrol and its receptor

Place the prepared RSIT-sensor in different concentrations of resveratrol solution, perform the Amperometry from low to high concentration, and select scanning potential of -0.38 V. The 60 s current value was selected as the steady-state current, and the current change rate before and after the receptor-ligand binding was plotted against the ligand concentration. Since the range of resveratrol concentration was wide and difficult to plot, the concentration was redefined:

$$\text{Let}: pCa = 14 + Log(C) \tag{2}$$

where, pCa represents resveratrol concentration after redefinition, and C denotes resveratrol concentration before redefinition. Equation (2) indicated that when pCa = 1, the minimum resveratrol concentration was 1×10^{-13} mol/L. The logarithmic values of resveratrol concentration were plotted on the abscissa, and the rate of change of the response current was plotted as ordinate (Fig. 4).

Due to the characteristics of electrochemical biosensors, the bare electrodes may also produce changes in current in

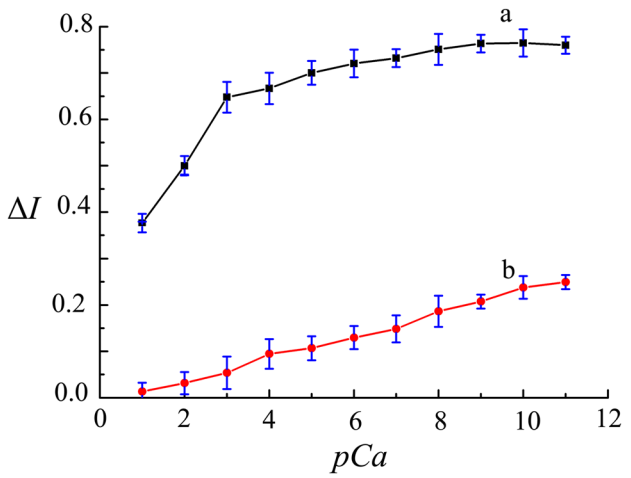

Fig. 4 Current response values of resveratrol in the detection range of 10^{-13} to 10^{-3} mol/L **a** Response curve of the RSIT-sensor to resveratrol **b** Response curve of bare electrode to resveratrol

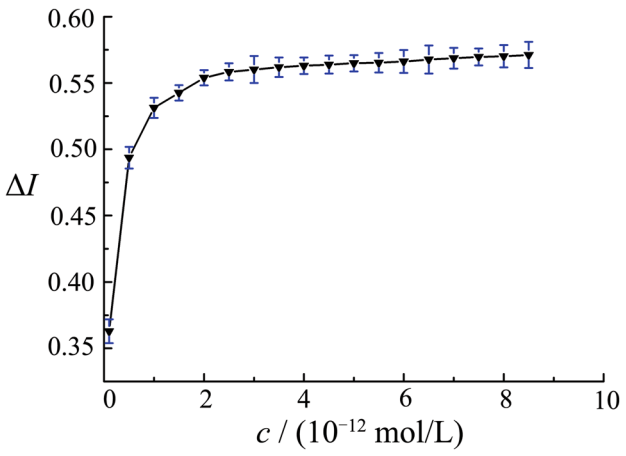

Fig. 5 Fitting of response curves for resveratrol in the concentration range of 10^{-13}-10^{-11} mol/L

different concentrations of resveratrol solution. The minimum response concentration of the bare electrode to resveratrol solution is 1×10^{-15} mol/L. In order to clarify the interaction between resveratrol and its receptors, it is highly essential to exclude the influence of bare electrodes on different concentrations of resveratrol solution. Therefore, the bare electrode was used to measure the current change rate of 10^{-13} to 10^{-3} mol/L resveratrol. As depicted in curve b in Fig. 4, after taking the logarithmic value of resveratrol concentration as X-axis, the rate of change of the response current was plotted on the ordinate as Y-axis. The rate of change of the response current of the bare electrode at different concentrations of resveratrol showed a satisfactory linear relationship.

In order to clarify the interaction between resveratrol and receptors, as shown in Fig. 4a, with the increase of resveratrol concentration, the current change rate first increased and then decreased, and the curve exhibited a parabolic characteristic, indicating that there was a resveratrol receptor on the intestinal cell membrane surface. Comparing the curves a and b in Fig. 4 unveiled that resveratrol could interact with corresponding receptors on intestinal epithelial cells. Through cell signal transmission and amplification, its response current could be remarkably improved, indicating a clear hyperbolic law. It is noteworthy that the signal is amplified by approximately 100 times (ratio of maximum response concentration (1×10^{-11} mol/L) to minimum response concentration (1×10^{-13} mol/L)). When the resveratrol concentration was 1×10^{-11} mol/L, the rate of change of the response current reached the maximum, indicating that the corresponding receptor on the intestinal epithelial cells has been saturated by the ligand. Besides, the rate of change of the response current significantly decreased when the concentration was increased, indicating that the intestinal epithelial cells were suppressed.

3.4 Kinetic curve presents the interaction between resveratrol and its receptors

As shown in Fig. 4, the rate of change of the response current showed a good linear relationship when the concentration of resveratrol was in the range of 10^{-13}-10^{-11} mol/L. Therefore, in that range, the concentration of detection was further subdivided into 20 gradients, namely 0.1, 0.5, 1.0, 1.5, 2.0, 2.5, 3.0, 3.5, 4.0, 4.5, 5.0, 5.5, 6.0, 6.5, 7.0, 7.5, 8.0, and 8.5 pmol/L. The resveratrol concentration was plotted on the abscissa and the rate of change of the response current was plotted on the ordinate. As shown in Fig. 5, the rate of change of the response current reached the maximum when the resveratrol concentration was 8.5 pmol/L, indicating that the receptor has been saturated with ligand.

In the range of 0.1–8.5 pmol/L resveratrol, the rate of change of the response current gradually increased with the elevation of the concentration, demonstrating that the correlation was remarkable (Fig. 5). The principle of interaction between receptors and ligands is similar to the kinetics of enzyme and substrate catalysis. In the low concentration range of 0.1 ~ 1 pmol/L, the rate of change of the response current linearly increased, indicating that the number of ligand molecules was remarkably lower than the number of corresponding receptors. In the high concentration range of 1 ~ 8.5 pmol/L, the rate of change of the response current was hyperbolic with elevation of concentration, indicating that the receptor was gradually saturated. The saturation concentration was 8.5 pmol/L. It can be speculated that the average number of receptors on the cell is about 85 based on the minimum detection limit and maximum saturation concentration of resveratrol. The fitting formula is given by:

$$\Delta I = \frac{0.571c}{0.1089 + c} \tag{3}$$

where, 0.571 is the maximum rate of change of the response current; 0.1089 is the concentration of resveratrol when the reaction reached half of the maximum rate of change of the response current (ΔI).

3.5 The binding constant and dissociation constant of resveratrol and its receptor

Set the test concentration of resveratrol in the range of $1.0\times10^{-13}\sim8.5\times10^{-12}$ mol/L in an increasing trend (0.1, 0.5, 1.0, 1.5, 2.0, 2.5, 3.0, 3.5, 4.0, 4.5, 5.0, 5.5, 6.0, 6.5, 7.0, 7.5, 8.0, and 8.5 pmol/L), and measure the corresponding steady-state current value for each additional concentration. Calculate the rate of change of the response current of each concentration according to Eq. (1). As depicted in Fig. 6, the reciprocal resveratrol concentration is plotted on the X-axis, and the reciprocal rate of change of the response current is plotted on the Y-axis.

$$\frac{1}{\Delta I} = 0.144\times10^{-12}\frac{1}{C} + 1.739\ \left(\mathrm{R}^2 = 0.997\right) \tag{4}$$

According to Eq. (4), the binding constant of the interaction between resveratrol and its receptor is given as follows: $Ka = 1.207 \times 10_{\circ}^{-11}$

Determine the steady-state value of the response current in an order from the highest concentration to the lowest, and calculate the rate of change of the response current (Fig. 7).

$$\frac{1}{\Delta I} = 0.846\times10^{-12}\frac{1}{C} + 0.946\ (\mathrm{R}^2 = 0.999) \tag{5}$$

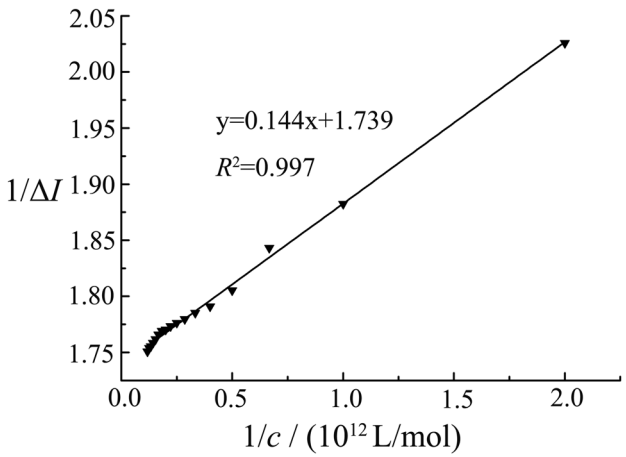

Fig. 6 Measurement of binding constant between resveratrol and its receptor

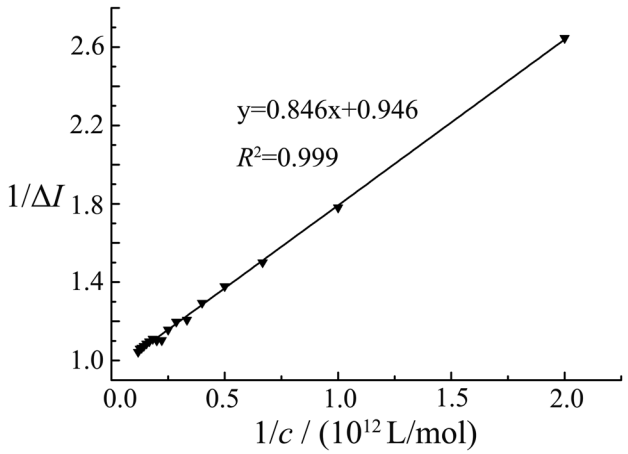

Fig. 7 Measurement of dissociation constant between resveratrol and its receptor

According to Eq. (5), the dissociation constant of the interaction between resveratrol and its receptor is presented as follows: $Kd = 1.118 \times 10_{\circ}^{-12}$

3.6 Stability and reproducibility of RSIT-sensor for resveratrol

The prepared RSIT-sensor was continuously measured 10 times in 10^{-12} mol/L resveratrol solution, and relative standard deviation (RSD) of the results was 7.34%, suggesting that stability of the RSIT-sensor was satisfactory. Then, the prepared RSIT-sensor was stored in saline at 4℃, and used to daily measure resveratrol with the same concentration. In the first two days, the rate of change of the response current was almost constant, while that was 75.6% in on the 4th day, indicating that the prepared RSIT-sensor could be stably stored for at the least two days. Five RSIT-sensors prepared in different batches were used to measure the same concentration of resveratrol solution. Results of current response are shown in Table 1, and the RSD of the response current was 7.97%, demonstrating that stability of the RSIT-sensors was acceptable.

Table 1 Results of the repeatability testing of RSIT-sensor

Sensor no	Responsive current (μA)	Blank current (μA)	ΔI
01	-0.1858	-0.2415	22.660
02	-0.4778	-0.6579	27.375
03	-0.1426	-0.1909	25.301
04	-0.2805	-0.3690	23.984
05	-0.3525	-0.4835	27.094

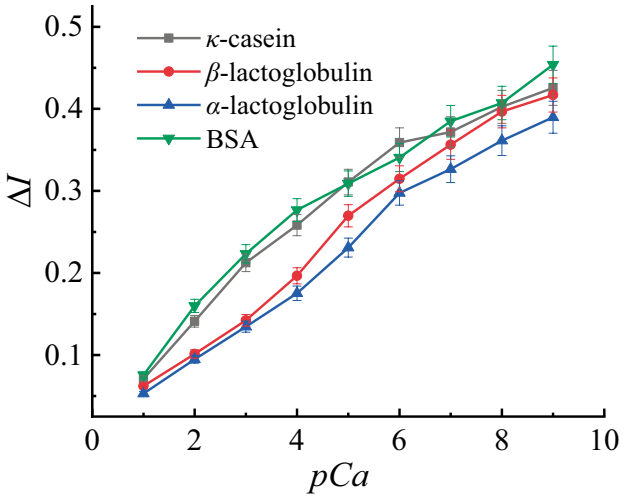

Fig. 8 Response currents of bovine serum albumin (BSA); α-lactoglobulin; β-lactoglobulin; κ-casein concentration range of 10^{-13} to 10^{-5} mol/L in the RSIT-sensor

3.7 Reaction kinetics between the RSIT-sensor and the nontarget compound

The RSIT-sensor was used to determine the current response of four bombykol analogues (bovine serum albumin (BSA 67 kDa); α-lactoglobulin (14.2 kDa); β-lactoglobulin (18.3 kDa); κ-casein (19 kDa)) in the concentration range of 10^{-13} mol/L to 10^{-5} mol/L. The logarithmic value of the corresponding compound concentration is plotted on the abscissa, and the current change rate of the response current is plotted on the ordinate Fig. 8. The relationship between the rate of current change and the compound concentration is linear rather than hyperbolic, indicating that the RSIT-sensor does not respond to these four compounds. The results show that the prepared sensor has good selectivity. However, the rat small intestine tissue sensor is a kind of biological tissue sensor. The receptors on the cell surface are very complicated. Therefore, it is impossible to perform specific measurement without directly knowing which receptor is responsible.

4 Conclusions

The RSIT-sensors prepared by immobilizing rat small intestinal epithelial cells were the first to quantitatively determine the interaction between resveratrol and its receptor with detection limit of 1×10^{-13} mol/L. The fitted hyperbolic model indicated that there was a resveratrol-related receptor on the small intestinal epithelial cells. With measurement of resveratrol at different concentrations, it can be concluded that the rate of change of the response current of resveratrol reached the maximum at the concentration of 8.5×10^{-12} mol/L. It highlighted that resveratrol-related receptor has been saturated. The binding constant and dissociation constant of resveratrol and its receptor were 1.207×10^{-11} and 1.118×10^{-12}, respectively. The action principle of resveratrol and its receptors is similar to the principle of enzyme–substrate catalytic kinetics. With comparing the response values of RSIT-sensor and bare electrode with resveratrol, the response value of small intestinal cells to resveratrol has obviously been amplified by the intracellular signal transmission system. The cell receptor clearly confers the saturability of the biosensor, which is similar to the typical characteristics of enzymatic reaction kinetics.

The RSIT-sensor simulates the signaltransduction process of small intestinal epithelial cells, successfullyquantitatively determines resveratrol, and explores its interaction with thecorresponding receptors. Our findings may provide new ideas for the study ofthe interaction between receptors and ligands. In addition, the biosensorexhibited a satisfactory stability and reproducibility, which increased theaccuracy and credibility of the experiment. However, whether the signaltransmission process of the small intestine tissue after being immobilized cantruly reflect the physiological characteristics of the small intestine needs tobe further studied.

Acknowledgments This study was financially supported by the National Natural Science Foundation of China (Grant No. 31901782).

Authors' contributions Ruijuan Ren participated in drafting the manuscript, as well as revision. Tingting Liu contributed to study design and drafting the primary version of the manuscript. The study was conducted under Dingqiang Lu's supervision. All authors have read and approved the submitted version of the manuscript.

Declarations

Conflict of interest The authors declare that there is no conflict of interest.

References

I. Ahmad, M. Hoda, Attenuation of diabetic retinopathy and neuropathy by resveratrol: Review on its molecular mechanisms of action. Life Sci **24515**, 117350 (2020)

J.M. Allaire, S.M. Crowley, H.T. Law, S.-Y. Chang, H.-J. Ko, B.A. Vallance, The intestinal epithelium: central coordinator of mucosal immunity. Trends Immunol. **39**(9), 677–696 (2018)

M. Athar, J.H. Back, L. Kopelovich, D.R. Bickers, A.L. Kim, Multiple molecular targets of resveratrol: Anti-carcinogenic mechanisms. Arch. Biochem. Biophys. **486**(215), 95–102 (2009)

N. Bostanghadiri, A. Pormohammad, A.S. Chirani, R. Pouriran, A. Hashemi, Comprehensive review on the antimicrobial potency of the plant polyphenol resveratrol. Biomed. Pharmacother. **95**, 1588–1595 (2017)

K.S. Bhullar, C.C. Udenigwe, Clinical evidence of resveratrol bioactivity in cardiovascular disease. Curr. Opin. Food. Sci. **8**, 68–73 (2016)

G.T. Diaz-Gerevini, G. Repossi, A. Dain, M.C. Tarres, M.D.F.A.M.S Undurti Narasimha Das, A.R. Eynard, Beneficial action of resveratrol: How and why? Nutrition **32**(2), 174–178 (2016)

M. Elshaer, Y. Chen, X.-J. Wang, X. Tang, Resveratrol: An overview of its anti-cancer mechanisms. Life Sci. **20715**, 340–349 (2018)

M. Jang, L. Cai, G.O. Udeani, K.V. Slowing, C.F. Thomas, C.W. Beecher, H.H. Fong, N.R. Farnsworth, A.D. Kinghorn, R.G. Mehta, R.C. Moon, J.M. Pezzuto, Cancer chemopreventive activity of resveratrol natural product derived from grapes. Science **275**, 218–200 (1997)

C.-W. Kim, K.-A. Hwang, K.-C. Choi, Anti-metastatic potential of resveratrol and its metabolites by the inhibition of epithelial-mesenchymal transition, migration, and invasion of malignant cancer cells. Phytomedicine **23**(14), 1787–1796 (2016)

S.S. Kulkarni, C. Cantó, The molecular targets of resveratrol. BBA-Mol. Basis Dis. **1852**(6), 1114–1123 (2015)

H. Li, N. Xia, U. Förstermann, Cardiovascular effects and molecular targets of resveratrol. Nitric Oxide **26**(2), 102–110 (2012)

M. Ligt, S. Timmers, P. Schrauwen, Resveratrol and obesity: Can resveratrol relieve metabolic disturbances? BBA-Mol. Basis Dis. **1852**(6), 1137–1144 (2015)

S.A.M. Martins, J.R.C. Trabuco, G.A. Monteiro, V. Chu, J.P. Conde, D.M.F. Prazeres, Towards the miniaturization of GPCR-based live-cell screening assays. Trends Biotechnol. **30**(11), 566–574 (2012)

R. Méjard, H.J. Griesser, B. Thierry, Optical biosensing for label-free cellular studies. TrAC, Trend Anal. Chem. **53**, 178–186 (2014)

M. Ndiaye, C. Philippe, H. Mukhtar, N. Ahmad, The grape antioxidant resveratrol for skin disorders: Promise, prospects, and challenges. Arch. Biochem. Biophys. **508**(215), 164–170 (2011)

M.R. Oliveira, S.F. Nabavi, A. Manayi, M. Daglia, Z. Hajheydari, S.M. Nabavi, Resveratrol and the mitochondria: from triggering the intrinsic apoptotic pathway to inducing mitochondrial biogenesis, a mechanistic view. BBA-Gen. Subjects **1860**(4), 727–745 (2016)

E. Öztürk, A.K.K. Arslan, M.B. Yerer, A. Bishayee, Resveratrol and diabetes: A critical review of clinical studies. Biomed. Pharmacother. **95**, 230–234 (2017)

M.M. Poulsen, K. Fjeldborg, M.J. Ornstrup, T.N. Kjær, M.K. Nøhr, S.B. Pedersen, Resveratrol and inflammation: challenges in translating pre-clinical findings to improved patient outcomes. BBA-Mol. Basis Dis. **1852**(6), 1124–1136 (2015)

L. Qiao, L. Jiao, G. Pang, J. Xie, A novel pungency biosensor prepared with fixing taste-bud tissue of rats. Biosens. Bioelectron. **68**, 454–461 (2015)

R. Ren, D. Lu, G. Pang, Development of a new and simple method for the detection of histidine-tagged proteins based on thionine-chitosan/gold nanoparticles/horseradish peroxidase. Biomed. Microdevices **22**(11), 1–10 (2020)

G. Repossi, U.N. Das, A.R. Eynard, Molecular basis of the beneficial actions of resveratrol. Arch. Med. Res. **51**(2), 105–114 (2020)

B.A. Sandoval-Ramírez, Ú. Catalán, A. Pedret, R.M. Valls, M.J. Motilva, L. Rubió, R. Solà, Exploring the effects of phenolic compounds to reduce intestinal damage and improve the intestinal barrier integrity: A systematic review of *in vivo* animal studies. Clin. Nutr. 2020, In Press

L. Subramanian, S. Youssef, S. Bhattacharya, J. Kenealey, A.S. Polans, P.R. van Ginkel, Resveratrol: challenges in translation to the clinic–a critical discussion. Clin. Cancer Res. **16**(24), 5942–5948 (2010)

H.Y. Tsai, C.T. Ho, Y.K. Chen, Biological actions and molecular effects of resveratrol, pterostilbene, and 3'-hydroxypterostilbene. J. Food Drug Anal. **25**(1), 134–147 (2017)

S. Ushiama, Y. Ishimaru, M. Narukawa, M. Yoshioka, C. Kozuka, N. Watanabe, M. Tsunoda, N. Osakabe, T. Asakura, H. Masuzaki, K. Abe, Catecholamines facilitate fuel expenditure and protect against obesity via a novel network of the gut-brain axis in transcription factor skn-1-deficient mice. Ebiomedicine **8**, 60–71 (2016)

A.J. Venkatakrishnan, X. Deupi, G. Lebon, C.G. Tate, G.F. Schertler, M.M. Babu, Molecular signatures of G-protein-coupled receptors. Nature **493**(7436), 185–194 (2013)

A. Vojdani, L.R. Gushgari, E. Vojdani, Interaction between food antigens and the immune system: Association with autoimmune disorders. Autoimmun. Rev. **19**(3), 102459 (2020)

L. Wei, L. Qiao, G. Pang, J. Xie, A kinetic study of bitter taste receptor sensing using immobilized porcine taste bud tissues. Biosens. Bioelectron. **92**, 74–80 (2017)

S. Xiao, Y. Zhang, P. Song, J. Xie, G. Pang, The investigation of allosteric regulation mechanism of analgesic effect using SD rat taste bud tissue biosensor. Biosens. Bioelectron. **126**, 815–823 (2019)

Q. Xu, D. Lu, G. Pang, Study on bombykol receptor self-assembly and universality of G protein cellular signal amplification system. ACS Sensors **4**, 257–264 (2019)

Y. Ye, H. Guo, X. Sun, Recent progress on cell-based biosensors for analysis of food safety and quality control. Biosens. Bioelectron. **126**, 389–404 (2019)